

See discussions, stats, and author profiles for this publication at: <https://www.researchgate.net/publication/222983745>

# Modelling studies of solvent effects on the conformational stability of agarobiose and neogarobiose and their relationship to agarose

ARTICLE *in* INTERNATIONAL JOURNAL OF BIOLOGICAL MACROMOLECULES · NOVEMBER 1989

Impact Factor: 2.86 · DOI: 10.1016/0141-8130(89)90018-4

---

CITATIONS

29

---

READS

7

4 AUTHORS, INCLUDING:



[Jesús Jiménez-Barbero](#)

Center for Cooperative Research in Biosciences

541 PUBLICATIONS 10,253 CITATIONS

SEE PROFILE



[Serge Perez](#)

French National Centre for Scientific Research - Grenoble Universit...

296 PUBLICATIONS 8,286 CITATIONS

SEE PROFILE

# Modelling studies of solvent effects on the conformational stability of agarobiose and neoagarobiose and their relationship to agarose

Jesus Jimenez-Barbero\*, Christine Bouffar-Roupe and Cyrille Rochas

Centre de Recherches sur les Macromolécules Végétales†, CNRS, 53X Grenoble Cédex, France

and Serge Pérez‡

Laboratoire de Physicochimie des Macromolécules, INRA, BP 527, 44026 Nantes Cédex, France

(Received 15 January 1989; revised 12 May 1989)

*The conformational equilibria of the low energy conformers of the repeating units of agarose, i.e. neoagarobiose and agarobiose have been studied theoretically in five solvents. The structure of each individual conformer has been refined by molecular mechanics calculations, from the distinct low-energy regions determined from potential energy surfaces. The stability of the conformers in dilute solution has been evaluated through consideration of the relaxed intramolecular energy including electrostatic, dispersion and cavity terms. For each disaccharide, the calculated abundance of conformers is practically independent of the solvent. Dipole moments and linkage rotation have been calculated for each of the low energy conformers. The calculated molar fractions of the stable conformers were used to model the optical rotation values measured for a single strand of agarose chain in its disordered state, and a satisfactory agreement has been reached ( $\Lambda_{\text{cal}} = -133^\circ$ ,  $\Lambda_{\text{obs}} = -145^\circ$ ). For the agarose molecule in the solid state, a left-handed threefold single helix, repeating in 2.85 nm is predicted. Such a helix, which represents the calculated stable conformation for a single strand of agarose, should be considered in descriptions of the molecular basis of sol-gel transition of agarose.*

**Keywords:** Conformation; agarobiose; neoagarobiose; agarose; optical rotation

## Introduction

The marine algal polysaccharides, agar and carrageenan, are extracted from those members of the *Rhodophyta* (red algae) known as agarophytes or carrageenophytes. They are well known for their ability to form gels and viscous solutions. For these reasons, they are widely used in food and other industrial processes as well as in biotechnology. Both agar and carrageenan are based on a residue of galactose with alternating  $\alpha(1\rightarrow3)$  and  $\beta(1\rightarrow4)$  links<sup>1,2</sup>. Specifically, the 4-O-linked sugars occur as the D-isomer in carrageenan; in agar, the 3,6-anhydro-galactopyranose or galactopyranose-6-sulphate occur as L-isomers. Agar is referred to more appropriately as a 'family of polysaccharides', the component having the greatest gelling tendency being agarose<sup>3</sup>.

In the solid state a double helix was first proposed for agarose by analogy with carrageenan<sup>3-6</sup>. The agarose double-helix has two parallel left-handed strands with threefold symmetry, a pitch of 1.9 nm, and an internal cavity of 0.45 nm<sup>6</sup>. This void is thought to be filled by water molecules involved in the stabilization of the double-helix through hydrogen bond formation<sup>7</sup>.

The gel-sol and sol-gel transitions of agarose are accompanied by sharp changes in optical rotation. This is believed to originate in cooperative transition from a random coil chain conformation in the high temperature state to the ordered double-helical conformation in the gel<sup>5,6</sup>. The transition shows marked thermal hysteresis between melting and setting; this is attributed to the stabilization of the double-helix structure, once formed, by extensive helix-helix aggregation. Another model for the gelation of agarose has been proposed by Atkins and Hill (in Ref. 8) in which agarose gels consist of 'fibrillar crystals composed of three-fold extended single helices of repeat distances 2.85 nm packed parallel to each other in one of three possible arrangements'<sup>8</sup>. Obviously, increased insight into the solution and solid state behaviour of agarose chains is needed.

One approach to the problem of polysaccharide conformation in solution is to consider related oligosaccharide fragments. The present report describes such a study using recently developed molecular modelling methods which have been applied previously to other carbohydrate systems with success<sup>9-12</sup>.

## Experimental

### Nomenclature

The idealized structure consists of alternating 1,3 linked  $\beta$ -D-galactopyranose and 1,4 linked 3,6-anhydro-

\* Permanent address: Instituto de Química Orgánica General, Juan de la Cierva, 3, Madrid-6, Spain.

† Affiliated to the 'Université Scientifique, Technologique et Médicale de Grenoble', Grenoble, France.

‡ To whom correspondence should be addressed.



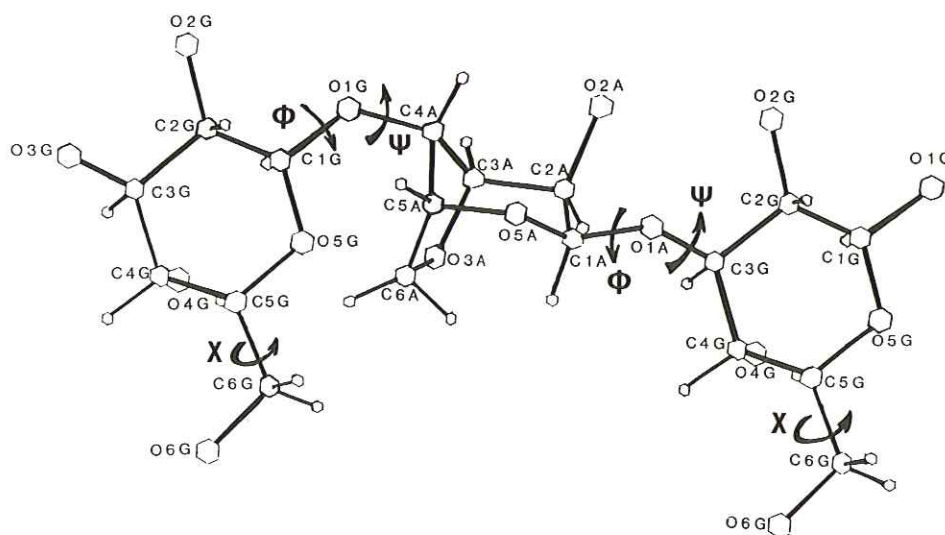


**Figure 1** Schematic representation of the basic trisaccharide unit of agarose, along with the labelling of the atoms and some torsion angles of interest

$\alpha$ -L-galactopyranose. In this idealized representation, agarose could be equally well defined as either a polymer of (1 $\rightarrow$ 3)- $\alpha$ -agarobiose or a polymer of (1 $\rightarrow$ 4)- $\beta$ -neoagarobiose. The schematic representation depicted in Figure 1 indicates the labelling of the atoms, and the torsional angles of interest. The atoms belonging to the galactopyranose units, are annotated by G and those of the anhydro-galactopyranose residue by a A.

The relative orientation of a pair of contiguous residues is described by the torsion angles  $\phi$  and  $\psi$ :

$$\phi_A = \text{O-5A} - \text{C-1A} - \text{O-1A} - \text{C-3G}$$

or

$$\phi_{H_A} = \text{H-1A} - \text{C-1A} - \text{O-1A} - \text{C-3G}$$

$$\psi_A = \text{C-1A} - \text{O-1A} - \text{C-3G} - \text{C-4G}$$

or

$$\psi_{H_A} = \text{C-1A} - \text{O-1A} - \text{C-3G} - \text{H-3G}$$

and

$$\phi_G = \text{O-5G} - \text{C-1G} - \text{O-1G} - \text{C-4A}$$

or

$$\phi_{H_G} = \text{H-1G} - \text{C-1G} - \text{O-1G} - \text{C-4A}$$

$$\psi_G = \text{C-1G} - \text{O-1G} - \text{C-4A} - \text{C-5A}$$

or

$$\psi_{H_G} = \text{C-1G} - \text{O-1G} - \text{C-4A} - \text{H-4A}$$

The exo-cyclic torsion angles  $\chi = \text{O-5G} - \text{C-5G} - \text{C-6G} - \text{O-6G}$ , define the orientation of the primary hydroxyl group of the galactopyranose residues. The orientations about  $\chi$  are also referred to as either *gauche-trans*, *gauche-gauche* or *trans-gauche*. In this terminology, the position of O-6 relative to O-5 is stated first, and the position of O-6 relative to C-4 second. The sign of the dihedral angles is defined according to the rules recommended by the IUPAC-IUB Commission of Biochemical Nomenclature<sup>13</sup>.

### Energy calculations

The preferred conformations and their energies were determined using three separate software systems of increasing complexity.

**Rigid-residue conformational analysis** For a given disaccharide moiety, the conformational energy is evaluated by including the partitioned contributions arising from van der Waals interactions, torsional and exo-anomeric potential, and inter-residue hydrogen bonding, using the PFOS computer program<sup>14</sup>. For this monomer coordinates for the  $\beta$ -D-galactopyranose residue in the  $^4C_1$  conformation were average values<sup>15</sup>, whereas those for the  $^1C_4$  conformation of the  $\alpha$ -L-anhydrogalactopyranose residue, were generated by taking the mirror image of the crystal structure of methyl-3,6-anhydro- $\beta$ -D-galactopyranoside<sup>16</sup>. In all instances, the coordinates of the hydrogen atoms attached to the carbon atoms were modified using a C-H bond length of 0.11 nm, and a bond vector appropriately set to the C-C and C-O vectors. Hydroxylic hydrogen atoms were not considered, and at this stage the ring geometry is considered as invariant. For each of the three low energy orientations of the primary hydroxyl group, the glycosidic torsional angles  $\phi$ ,  $\psi$  were stepped in increments of  $5^\circ$  over the whole angular range from  $-180^\circ$  to  $180^\circ$ . With respect to the energy minimum, the iso-energy contours were drawn by interpolation at 1 kcal/mol intervals; the 10 kcal/mol contour was selected as the outer limit. Such a map is referred to as the 'rigid map'.

**Refinement of minimum with relaxed residue calculations** Each low energy conformer resulting from the PFOS calculation was submitted to energy optimization by the MM2CARB method. MM2CARB is the MM2 force-field program<sup>17</sup> (Quantum Chemistry Program Exchange no. 395) modified with the acetal-segment (C-5-O-5-C-1-O-1-C-x) parameters of Jeffrey and Taylor<sup>18</sup>. As already demonstrated, these parameters reproduce, in an adequate fashion, the dependence of geometry upon variations of glycosidic torsion angles, as observed in carbohydrate structures<sup>19</sup>.



Contributions arising from stretching, bending, stretch-bending, torsional, dipolar and non-bonded energies are taken into account. In such a type of calculation, all the atoms, including the hydroxylic hydrogen atoms, as well as the lone pairs on the oxygen atoms have to be considered.

**Solvated energy** In the 'continuum' theory the conformational free energy of a given disaccharide conformer in a particular solvent ( $G_T$ ) is composed of the energy of the isolated molecule ( $G_H$ ) and the solvation free energy<sup>9,20</sup> ( $G_{solv}$ ):

$$G_T = G_H + G_{solv}$$

In the method used to evaluate solvation energy, the process of dissolving a molecule in a solvent involves two steps. The first step is the creation of a cavity in a solvent of suitable size to accommodate the solute molecule in the given conformation. The cavity formation requires a Gibbs free energy  $G_{cav}$ . The second step is the introduction into this cavity of the solute molecule which interacts with the surrounding solvent molecules. The interaction part of the solvation free energy  $G_{solv}$  is composed of the free energy of dispersion  $G_{disp}$  and electrostatic  $G_{elect}$  interactions of solute molecules with the solvent. The solvation energy is the sum of three contributions: the cavity term, electrostatic interactions, and dispersion interactions:

$$G_{solv} = G_{cav} + G_{elect} + G_{disp}$$

Expressions for the calculation of individual contributions to the solvation energy, as well as the physicochemical parameters characterizing the solvents, have been presented elsewhere<sup>9,20</sup>. The hard-sphere radius of the solute is calculated from the van der Waals volumes<sup>21</sup> and all parameters characterizing the solvation energy terms, except for index of refraction ( $n = 1.56$ ) are the calculated PCILO values. PCILO is the semi-empirical Perturbative Configuration Interaction with Localized Orbitals quantum chemical method<sup>22</sup> using the Powell-Zangwill algorithm<sup>23,24</sup>.

#### Calculation of optical rotation

The optical activity of oligo- and polysaccharides, measured at a single wavelength (usually at the sodium D-line at 589 nm) has also been shown to be sensitive to chain conformation. The total optical activity arises not only from the structure and conformation of individual carbohydrate moieties, along with their configuration at the anomeric centres, but also from the torsion angles about the glycosidic linkage. The contribution from the linkage rotation  $\Lambda$  is decomposed into basic components<sup>25,26</sup>. The mean value of  $\Lambda$  is readily computed using Boltzman's probability of conformers in a given solvent. From the observed  $[\alpha]_D$  line specific rotation, the linkage rotation  $|\Lambda|$  is defined as follows:

$$|\Lambda| = |M| - |A| - |G| = -120(\sin \phi^H + \sin \psi^H)$$

where

$$|A| = -42^\circ, \text{ is the molar rotation of } 3,6\text{-}\alpha\text{-L-anhydrogalactopyranose}$$

$$|G| = 95^\circ, \text{ is the molar rotation of } \beta\text{-D-galactopyranose}^{27}$$

and

$$|M| = |\alpha|_D \times m/100,$$

where  $m$  is the molecular weight of the repeating disaccharide.

#### Measurement of optical rotation

The optical rotation was measured at 589 nm on a Perkin-Elmer 241 polarimeter using thermostatically regulated cells of 10, 20 or 100 mm pathlength. The sample of agarose was supplied by Marine Colloids. The sulphate content was 0.3% as verified by different techniques<sup>28</sup>. The specific rotation of the coil form was found to be  $-30^\circ$ , irrespective of the concentration in the range 0.48 to 31.0 g/l. In the same range of concentrations, the specific rotation of the helical form was  $-49^\circ$  at  $4^\circ\text{C}$ . From the experimental value of the specific rotation, the sign and the magnitude of the linkage rotation  $\Lambda$  can be easily computed. They are  $\Lambda = -145^\circ$  and  $\Lambda = -201^\circ$  for the coil form and the helical form, respectively.

#### Helical parameters

Helical arrangements are customarily described in terms of a set of helical parameters: ( $n, h$ ),  $n$  being the number of residues per turn of the helix, and  $h$  being the translation of the corresponding residues residue along the helix axis. With set values of glycosidic valence angles and residue geometry, these parameters can be calculated for any given value of the sets of glycosidic torsional angles:  $\phi_A, \psi_A, \phi_G, \psi_G$ , following an algorithm already reported<sup>29</sup>.

#### Results and discussion

The rigid maps for the agarobiose and neoagarobiose disaccharides are shown respectively in *Figures 2* and *3*. On each map, the locations of all the low energy conformers are indicated. The molecular drawings associated with each of the individual stable conformations are shown in *Figures 4* and *5*. The relative PFOS energies for the stable conformers of agarobiose and neoagarobiose, depending on the conformation of the primary hydroxyl group and on the occurrence of inter-residue hydrogen bonding have been computed. In the case of neoagarobiose, six energy minima are found: AG1( $-170^\circ, 90^\circ$ ), AG2( $-90^\circ, 50^\circ$ ), AG3( $-110^\circ, -70^\circ$ ), AG4( $-80^\circ, 150^\circ$ ), AG5( $30^\circ, 130^\circ$ ) and AG6( $-50^\circ, 160^\circ$ ). Four of these relative orientations of residues allow formation of intramolecular hydrogen bonds. For AG1, AG4 and AG5, the stabilizing energy of hydrogen bonding may be influential; AG2 has the lowest energy and corresponds to the formation of one hydrogen bond between O-5A and O-4G. Similar conclusions can be drawn for the agarobiose. Five low energy conformers can be identified: GA1( $-180^\circ, 160^\circ$ ), GA2( $-90^\circ, 180^\circ$ ), GA3( $-80^\circ, -80^\circ$ ), GA4( $60^\circ, -140^\circ$ ) and GA5( $10^\circ, 180^\circ$ ). GA1 is the only one which allows the formation of an intramolecular hydrogen bond between O-2G and O-2A. For both disaccharides orientation of the primary hydroxyl group does not seem to have any major influence on the occurrence and the relative energy of the stable conformers.

Each of these low energy conformers was optimized with MM2CARB. For each conformer, the exocyclic



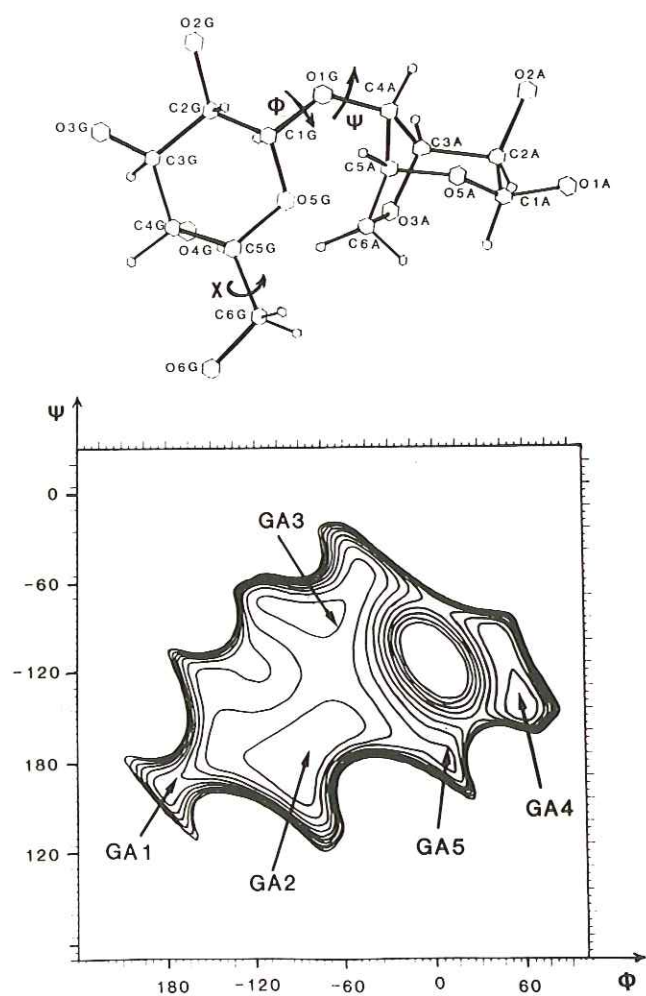


**Figure 2** Two-dimensional iso-energy map ( $\phi, \psi$ ) for agarobiose. With respect to the global minimum, the iso-energy contours are drawn by interpolation of 1 kcal/mol

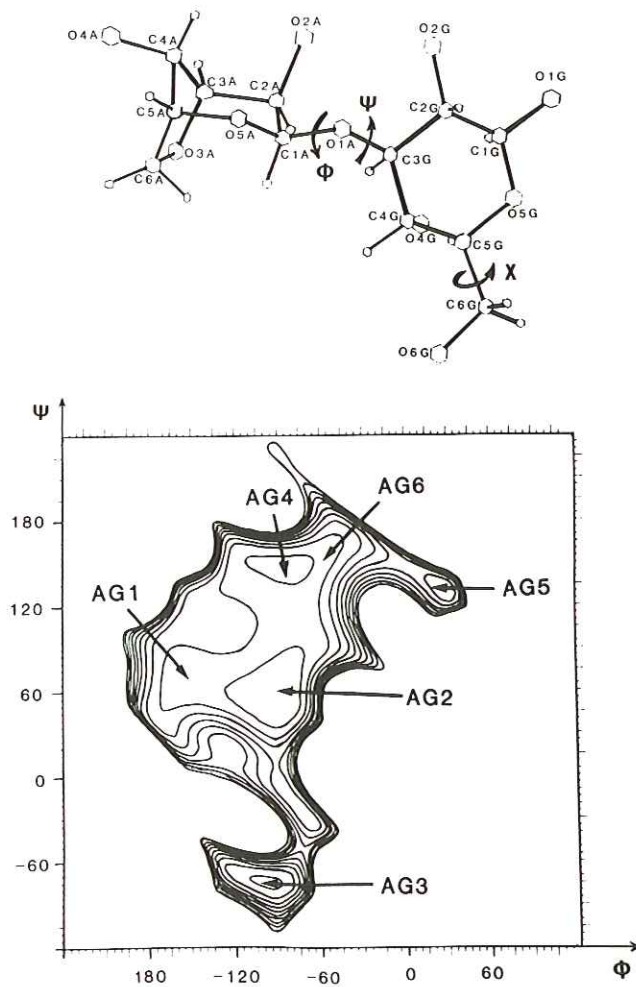


**Figure 3** Two-dimensional iso-energy map ( $\phi, \psi$ ) for neoagarobiose. With respect to the global minimum, the iso-energy contours are drawn by interpolation of 1 kcal/mol

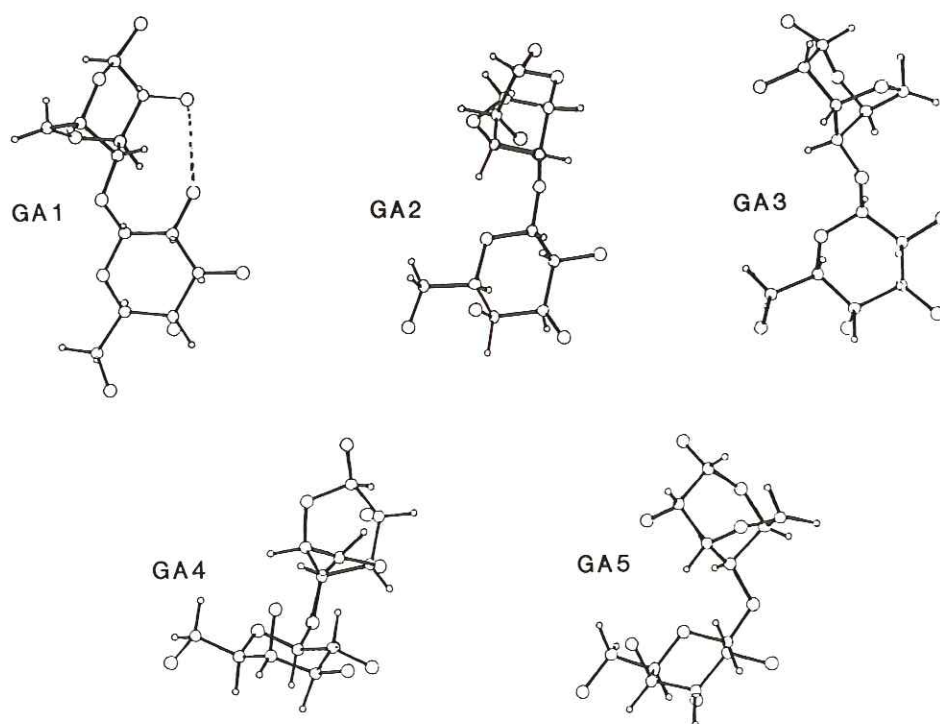


**Figure 4** Molecular drawing of the five stable conformers of agarobiose (PITMOS, Ref. 32). For the sake of simplification, the hydroxylic hydrogen atoms are not represented; hydrogen bonds are shown as broken lines

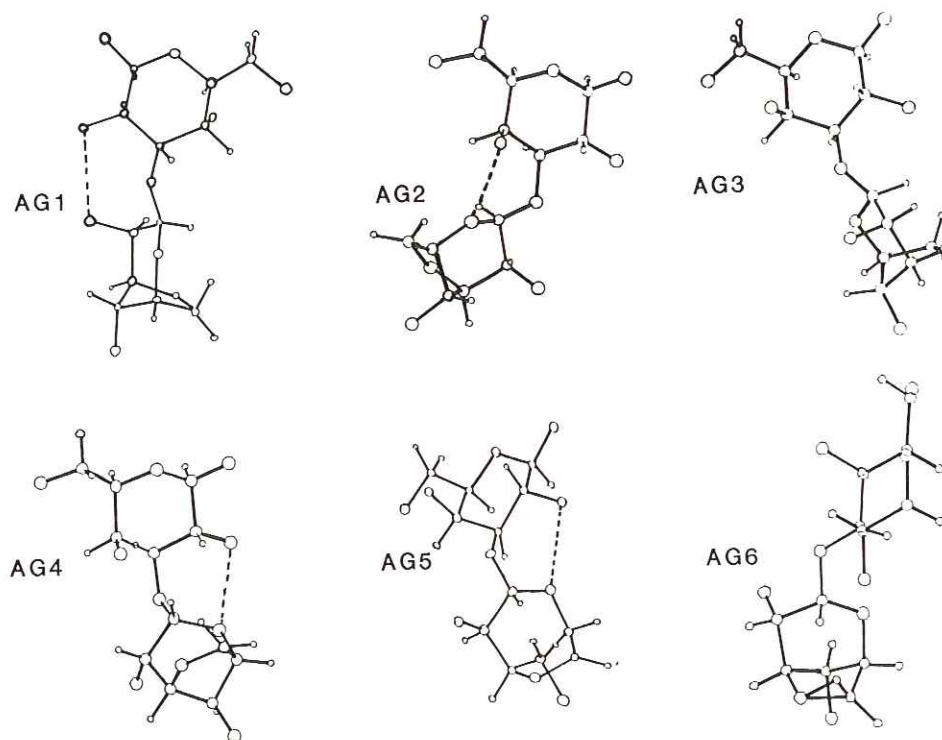


**Figure 5** Molecular drawing of the five stable conformers of neoagarobiose (PITMOS, Ref. 32). For the sake of simplification, the hydroxylic hydrogen atoms are not represented; hydrogen bonds are shown as broken lines

**Table 1** Relative  $E_{\text{MM2CARB}}$  energies<sup>a</sup> (kcal/mol) and geometrical features of the five stable conformers of 3,6-anhydro-4-*O*-( $\beta$ -D-galactopyranosyl)- $\alpha$ -L-galactopyranose (GA) and of the six stable conformers of 3-*O*-(3,6-anhydro- $\alpha$ -L-galactopyranosyl)- $\beta$ -D-galactopyranose (AG) together with values of expected interglycosidic proton-proton distances  $r$ , linkage rotations  $\Lambda$ , and dipole moments  $\mu$

	$E_{\text{MM2CARB}}$	$\mu(\text{D})$	$r(\text{\AA})$	$\phi(^{\circ})$	$\psi(^{\circ})$	$\phi^{\text{H}}(^{\circ})$	$\psi^{\text{H}}(^{\circ})$	$\Lambda(^{\circ})$
AG1	2.18	2.15	2.70	-163.8	80.3	-53.3	-42.9	177.6
AG2	0.00	2.97	2.23	-77.2	60.3	40.0	-61.9	28.8
AG3	2.65	3.25	3.56	-78.8	-87.8	37.8	159.9	-114.0
AG4	1.50	2.35	2.42	-63.5	141.5	52.6	23.8	-142.8
AG5	3.68	5.22	3.42	53.0	126.7	163.4	5.3	-45.6
AG6	1.73	1.81	2.86	-51.9	161.4	64.8	46.1	-194.4
GA1	3.73	1.98	3.30	179.1	164.6	-70.8	-75.5	229.2
GA2	0.92	2.31	2.24	-79.3	177.1	39.3	-62.5	31.2
GA3	0.00	2.93	2.65	-64.6	-87.2	53.1	42.0	-176.4
GA4	1.17	1.86	3.43	59.9	-140.0	172.4	-17.3	20.4
GA5	1.66	2.17	3.06	10.5	178.5	124.9	-60.8	6.0

<sup>a</sup> *Trans-gauche* conformation

torsion angle  $\chi$  was systematically started in the three non-eclipsed conformations, and the least energetic structure was sought. The *trans-gauche* orientation consistently yielded the lowest energies. Therefore, this orientation was selected for the rest of the work. In the case of AG2, the optimization of the geometry which was started from the *gauche-trans* orientation gave the *trans-gauche* one upon completion of the refinement. Table 1 shows calculated optimal values of torsional angles  $\phi$  and  $\psi$  for the six neoagarobiose minima and for the five agarobiose minima, along with estimated values of the linkage rotation  $\Lambda$ , and the distance of glycosidic protons  $r$ . MM2CARB calculated energies  $E$ , and dipole moments  $\mu$  are also included. All the refined conformations remain in the vicinity of the starting values; the largest displacement being found for AG3. For neoagarobiose,

the global energy minimum is AG2 ( $\phi_{\text{A}} = -77.2^{\circ}$ ,  $\psi_{\text{A}} = 60.3^{\circ}$ ); AG3 ( $\phi_{\text{G}} = -64.6^{\circ}$ ,  $\psi_{\text{G}} = -87.2^{\circ}$ ) being the global energy minimum for agarobiose. These values of the  $\phi$  torsion angle are in agreement with the stabilizing influence of the *exo-anomeric* effect.

Molar fractions of stable neoagarobiose and agarobiose conformers were estimated from the calculated values of the free-energy differences in the isolated state and in five solvents (Table 2). Based upon the MM2CARB energies, the distribution of conformers for the isolated neoagarobiose and agarobiose is AG2 > AG4 > AG6 > AG1 > AG3 > AG5 and GA3 > GA2 > GA4 > GA5 > GA1. Based upon the calculated PCILO energies, the distribution of conformers for agarobiose is identical, whereas the neoagarobiose one is slightly different (AG2 > AG4 > AG6 > AG3 > AG1 >



**Table 2** Relative energies  $E$  for the optimized conformers<sup>a</sup> of AG and GA in vacuum and in different solvents

	$E$ (kcal/mol)					
	$E_{\text{vacuum}}$	$E_{\text{dioxane}}$	$E_{\text{pyridine}}$	$E_{\text{methanol}}$	$E_{\text{DMSO}}$	$E_{\text{water}}$
AG1	2.18	2.18	2.32	2.47	2.38	2.73
AG2	0.00	0.00	0.00	0.00	0.00	0.00
AG3	2.65	2.60	2.58	2.57	2.58	2.52
AG4	1.50	1.59	1.74	1.89	1.79	2.22
AG5	3.68	3.23	2.59	2.17	2.54	1.06
AG6	1.73	1.86	2.10	2.39	2.26	2.96
GA1	3.73	3.88	4.00	4.02	3.93	4.24
GA2	0.92	1.03	1.15	1.17	1.09	1.36
GA3	0.00	0.00	0.00	0.00	0.00	0.00
GA4	1.17	1.27	1.41	1.53	1.44	1.81
GA5	1.66	1.79	2.03	1.91	1.83	2.10

<sup>a</sup> *Trans-gauche* conformation**Table 3** Solvation free energy (kcal/mol) of stable conformers<sup>a</sup> in selected solvents and a decomposition into individual contributions

		AG1	AG2	AG3	AG4	AG5	AG6	GA1	GA2	GA3	GA4	GA5
<i>p</i> -Dioxane	$G_{\text{el}}$	-0.13	-0.23	-0.24	-0.12	-0.69	-0.07	-0.06	-0.07	-0.17	-0.07	-0.07
	$G_{\text{cav}}$	5.20	5.19	5.19	5.20	5.24	5.25	5.19	5.19	5.24	5.23	5.19
	$G_{\text{disp}}$	-33.57	-33.47	-33.50	-33.49	-33.50	-33.54	-33.48	-33.51	-33.56	-33.56	-33.59
	$G_{\text{solv}}$	-28.50	-28.50	-28.55	-28.41	-28.95	-28.37	-28.35	-28.39	-28.50	-28.40	-28.37
Pyridine	$G_{\text{el}}$	-0.32	-0.46	-0.58	-0.29	-1.67	-0.17	-0.15	-0.17	-0.40	-0.16	-0.17
	$G_{\text{cav}}$	6.80	6.79	6.79	6.80	6.86	6.86	6.78	6.79	6.85	6.84	6.78
	$G_{\text{disp}}$	-28.58	-28.48	-28.52	-28.51	-28.52	-28.56	-28.49	-28.52	-28.48	-28.47	-28.51
	$G_{\text{solv}}$	-22.10	-22.24	-22.31	-22.00	-23.33	-21.87	-21.86	-21.90	-22.13	-21.89	-21.89
Methanol	$G_{\text{el}}$	-0.48	-0.82	-0.87	-0.43	-2.44	-0.26	-0.22	-0.26	-0.60	-0.24	-0.25
	$G_{\text{cav}}$	13.35	13.33	13.33	13.35	13.46	13.46	13.31	13.33	13.44	13.44	13.32
	$G_{\text{disp}}$	-21.11	-21.03	-21.06	-21.05	-21.04	-21.08	-21.04	-21.06	-21.09	-21.09	-21.05
	$G_{\text{solv}}$	-8.23	-8.52	-8.60	-8.13	-10.03	-7.86	-7.95	-7.99	-8.24	-7.89	-7.99
DMSO	$G_{\text{el}}$	-0.36	-0.62	-0.66	-0.33	-1.87	-0.19	-0.17	-0.20	-0.45	-0.18	-0.19
	$G_{\text{cav}}$	17.74	17.71	17.70	17.73	17.88	17.89	17.68	17.71	17.85	17.84	17.68
	$G_{\text{disp}}$	-23.75	-23.67	-23.69	-23.69	-23.72	-23.75	-23.67	-23.70	-23.76	-23.76	-23.68
	$G_{\text{solv}}$	-6.38	-6.58	-6.65	-6.29	-7.70	-6.05	-6.16	-6.19	-6.36	-6.09	-6.19
Water	$G_{\text{el}}$	-0.92	-1.53	-1.62	-0.82	-4.36	-0.49	-0.42	-0.50	-1.10	-0.44	-0.48
	$G_{\text{cav}}$	19.58	19.55	19.54	19.58	19.75	19.76	19.52	19.55	19.71	19.70	19.52
	$G_{\text{disp}}$	-24.29	-24.20	-24.24	-24.22	-24.18	-24.22	-24.22	-24.24	-24.25	-24.25	-24.23
	$G_{\text{solv}}$	-5.63	-6.18	-6.31	-5.46	-8.80	-4.95	-5.12	-5.19	-5.63	-4.99	-5.19

<sup>a</sup> *Trans-gauche* conformation

AG5). A table containing the PCILO net charges on the atoms for each of the stable conformers has been deposited. The results given in Table 2 indicate that the equilibrium compositions of both types of disaccharide do not depend strongly on the solvent. Individual components of solvation energy for five solvents are given in Table 3; none show any strong conformational dependence. For a given solvent, the cavity term remains practically constant. The strongest differences among the low energy conformers are found for the electrostatic contribution in the case of solvent of increasing polarity. The electrostatic term follows approximately the conformational dependence of the dipole moment. Nevertheless, the magnitude of such differences is never large enough to rearrange the ranking of the conformer established by MM2CARB or PCILO calculations on the isolated molecules. In previous studies, marked differences in the solvent effect of aqueous and non-aqueous solutions were observed in the case of maltose<sup>9</sup>,

cellobiose<sup>10</sup> and mannobiose<sup>11</sup>. Therefore, the lack of differences between solvent-induced conformational changes seems to be a distinct feature of agarobiose and neoagarobiose.

Taking into account the calculated molar fractions of the six stable conformers of neoagarobiose, and the five stable conformers of agarobiose, in water at 25°C, the mean value of the linkage rotation is  $-133^\circ$ . This can be compared to the experimentally derived values of  $-144^\circ$  from the specific rotation of the coil and  $-149^\circ$  from the specific rotation of the oligomers<sup>30</sup>. There is therefore, an excellent agreement between the observed and calculated values of the linkage rotation  $\Lambda$ . This indicates that the disordered state of agarose chains, in aqueous solution, is conveniently described by the dynamical average of the six conformations about the (1→4) linkage and the five conformations about the (1→3) linkage. It has to be stressed that in this so-called random coil, the agarose chain spends most of its time oscillating about



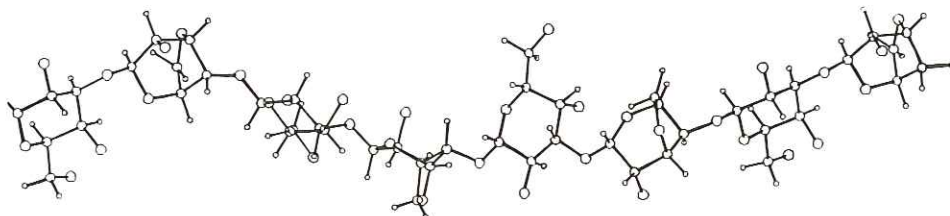


**Figure 6** Molecular drawing (PITMOS, Ref. 32) of the most stable single chain of agarose, having a left-handed threefold symmetry and a fibre repeat of 2.85 nm

**Table 4** Atomic coordinates in angles of the disaccharide unit corresponding to the helical conformation  $n = -3$ ;  $h = 9.5$  Å of the agarose chain

Atom	x	y	z
O1(A)	0.99694	1.64304	5.10784
C1(A)	0.12100	2.13488	4.16499
C2(A)	0.91128	3.03365	3.20716
C3(A)	0.08960	3.16745	1.91986
C4(A)	-0.12139	1.81450	1.28653
C5(A)	-1.17066	1.32100	2.27723
C6(A)	-2.06461	2.54060	2.41968
O2(A)	2.18004	2.46023	2.86636
O3(A)	-1.19190	3.68136	2.23455
O4(A)	-0.73241	1.91473	0.00000
O5(A)	-0.47230	0.99008	3.50291
H1(A)	-0.67206	2.85235	4.41997
H2(A)	0.87552	4.06984	3.57630
H3(A)	0.62927	3.81375	1.21238
H4(A)	0.62880	1.01360	1.26314
H5(A)	-1.54632	0.33975	1.94325
H61(A)	-3.08409	2.27941	2.10399
H62(A)	-1.96876	3.10244	3.32850
C1(G)	0.96242	0.19040	8.55627
C2(G)	1.53732	0.73943	7.25974
C3(G)	0.42216	1.13652	6.30344
C4(G)	-0.54339	-0.02576	6.10988
C5(G)	-1.01236	-0.55471	7.45955
C6(G)	-1.88756	-1.78470	7.33885
O2(G)	2.37256	1.85290	7.54984
O4(G)	0.10890	-1.09827	5.37297
O5(G)	0.11448	-0.92414	8.27001
O6(G)	-3.03757	-1.52021	6.54948
H1(G)	0.38028	0.95256	9.10095
H2(G)	2.12407	-0.04966	6.76884
H3(G)	-0.41923	1.81024	6.52108
H4(G)	-1.33862	0.28208	5.41444
H5(G)	-1.52546	0.25456	8.00583
H61(G)	-1.26762	-2.63493	7.01494
H62(G)	-2.33592	-2.00397	8.31380

conformations of the type AG2 and GA3 as shown by the population of the conformers.

It is also straightforward to generate chains having an helical propagation based on the regular alternation of AG2 and GA3 type of conformers. The resulting conformation is characterized by a set of helical parameters:  $n = -3.0$  and  $h = 0.95$  nm; this corresponds to a left-handed threefold single chain, having a fibre repeat of 2.85 nm. The value of the linkage rotation would be  $\Lambda = -147.6^\circ$ . A molecular drawing of such an extended helix is shown in Figure 6. The atomic coordinates of the repeating unit having this conformation are listed in Table 4. This helix is similar to

the one proposed by Atkins and Hill in 1981<sup>8</sup>. Such a helix, which represents the calculated stable conformation for a single strand of agarose, should be considered in descriptions of the molecular basis of sol-gel transition of agarose.

A double helical structure was proposed after a fibre diffraction analysis by Arnott *et al.*<sup>6</sup>, who observed a 0.95 nm spacing, plus meridional reflections on the third and sometimes on the first layer lines. The meridional reflection on the first layer line was considered as indicating that some of the scattering material had a lower symmetry. This led to the discarding of stable single-chain models having the observed helical parameters. Instead, multi-stranded helices were considered of which the parallel double helix having its strands related by an axial translation of half the single chain pitch was selected. The final model selected by Arnott *et al.*<sup>6</sup> contained two intertwined left-handed helices, having:  $n = -3$  and  $h = 0.634$  nm. In this model the glycosidic torsion angles are  $\phi_A = -52^\circ$ ,  $\psi_A = 156^\circ$  and  $\phi_G = -123^\circ$ ,  $\psi_G = -113^\circ$ .

In the case of alternating polysaccharides, the assignment of stable conformations in agreement with observed helical parameters is a complicated matter. Using the algorithm described previously<sup>29</sup>, the two surfaces for agarose corresponding to iso- $n = 3$ , iso- $h = 0.634$  nm and to iso- $n = -3$ , iso- $h = 0.634$  nm were produced. The maps were computed by incrementing  $\phi$  and  $\psi$  torsion angles. For each combination of  $\phi_A$ ,  $\psi_A$ , the numerical values of  $\phi_G$  and  $\psi_G$  consistent with the helical parameters were analytically evaluated. Only the combinations of  $\phi_A$ ,  $\psi_A$ ,  $\phi_G$  and  $\psi_G$  belonging to the allowed energy regions were kept; the corresponding value of the linkage rotation was computed (Table 5). Only 12 combinations of the four glycosidic torsion angles can give rise to the observed set of helical parameters. Four of them would generate right-handed threefold helices whereas eight would correspond to a left-handed chirality. However, only two models would give values of the linkage rotation ( $\Lambda = -196^\circ$  and  $\Lambda = -201^\circ$ ) in a close agreement with the one measured on agarose in the ordered form of  $\Lambda = -201^\circ$ . Only one right-handed model has a value within  $50^\circ$  of the experimental one. (This is assuming that the ordered conformation that exists in the gel junctions zones is closely related to the one which is present in the oriented samples from which the X-ray diffractogram was recorded.) The two left-handed models have values of the glycosidic torsion angles: ( $\phi_A = -80^\circ$ ,  $\psi_A = 150^\circ$ ); ( $\phi_G = -130^\circ$ ,  $\psi_G = -84^\circ$ ) and ( $\phi_A = -52^\circ$ ,  $\psi_A = 161^\circ$ ); ( $\phi_G = -115^\circ$ ,  $\psi_G = -125^\circ$ ). These have to be compared to the ones in the final model selected by Arnott *et al.*<sup>6</sup>: ( $\phi_A = -52^\circ$ ,  $\psi_A = 156^\circ$ ) and ( $\phi_G = -123^\circ$ ,  $\psi_G = -113^\circ$ ).



**Table 5** Combinations of the four glycosidic angles, generating helical structures having  $n = -3$  and  $h = 0.634$  nm (nos 1 to 8) and  $n = 3$  and  $h = 0.634$  nm (nos 9 to 12), along with the corresponding value of the linkage rotation  $\Lambda$ 

	$\phi G$	$\psi G$	$\phi A$	$\psi A$	$\Lambda$
1	-130	-84	-80	150	-195.6
2	55	-110	-170	90	30.0
3	-90	168	25	130	-68.0
4	60	-140	-140	83	50.4
5	10	180	-128	170	81.0
6	60	-140	-108	47	85.6
7	180	160	-105	-90	177.0
8	-115	-125	-52	161	-201.6

	$\phi G$	$\psi G$	$\phi A$	$\psi A$	$\Lambda$
9	-80	-80	-80	-90	60.0
10	180	160	-90	127	92.4
11	25	155	-105	-70	-34.8
12	-110	-72	-105	-70	-144.0

However, whereas these conformations are sterically acceptable (Figures 2 and 3) none of them corresponds to any of the stable orientations computed for the disaccharide units. Nevertheless, since no interchain interactions which might possibly stabilize the double helix were taken into consideration, no definite conclusion about the high energy of this double helix can be drawn.

## Conclusions

The present work was conducted on the idealized structure of agarose. It was performed with a series of modelling procedures which all showed that several low energy conformers have to be taken into account. The equilibrium between these conformational states remains practically constant upon changes of the solvent. The calculated molar fractions of the stable conformers in water were used to compute optical rotation values. The agreement between the calculated and the experimental data is satisfactory. In addition to gaining an understanding of the disordered state of the agarose chain some insights into stable single chains have been made possible. A left-handed threefold single helix, repeating in 0.285 nm, has been shown to be the most stable form. It should certainly be considered as an intermediate from occurring in the sol-gel transition of agarose. A similar conclusion was reached for carrageenan<sup>31</sup>. It has to be

emphasized that all these conclusions, which relate to experimentally observed features and behaviour of single chains, have been reached through calculations and the sole knowledge of the primary structure. The results which have been obtained will form a basis for further modelling of the association of multiple chains.

## Acknowledgement

Financial support for the stay of one of us (J.J.B.) was provided by the Centre National de la Recherche Scientifique.

## References

- Araki, C. *Bull. Chem. Soc. Jpn.* 1956, **29**, 543
- Araki, C. and Arai, K. *Bull. Chem. Soc. Jpn.* 1967, **40**, 1452
- Rees, D. A. *Adv. Carbohydr. Chem. Biochem.* 1969, **24**, 267
- Rees, D. A., Steele, I. W. and Williamson, F. B. *J. Polym. Sci.* 1969, **Part C**, 261
- Dea, I. C. M., McKinnon, A. A. and Rees, D. A. *J. Mol. Biol.* 1972, **68**, 153
- Arnott, S., Fulmer, A., Scott, W. E., Dea, I. C. M., Moorhouse, R. and Rees, D. A. *J. Mol. Biol.* 1974, **90**, 269
- Corongiu, G., Fornili, S. L. and Clementi, E. *Int. J. Quant. Chem.* 1983, **10**, 277
- Letherby, M. and Young, D. A. *J. Chem. Soc., Faraday Trans. I*, 1981, **77**, 1953
- Tvaroska, I. *Biopolymers* 1982, **21**, 1887
- Tvaroska, I. *Biopolymers* 1984, **23**, 1951
- Tvaroska, I., Pérez, S., Noble, O. and Taravel, F. *Biopolymers* 1987, **26**, 1499
- Jimenez-Barbero, J., Noble, O., Pfeffer, O. and Pérez, S. *New J. Chem.* 1989, **12**, 941
- IUPAC-IUB Commission on Biochemical Nomenclature. *Arch. Biochem. Biophys.* 1971, **145**, 405
- Pérez, S., Thèse de Doctorat d'Etat, 1978, Université de Grenoble, France
- Sheldrick, B. and Akridge, D. *Acta Crystallogr.* 1980, **B36**, 1615
- Campbell, J. W. and Harding, M. M. *J. Chem. Soc., Perkin Trans. II*, 1972, 1721
- Allinger, N. L. *J. Am. Chem. Soc.* 1977, **99**, 8127
- Jeffrey, G. A. and Taylor, R. J. *Comp. Chem.* 1980, **1**, 99
- Tvaroska, I. and Pérez, S. *Carbohydr. Res.* 1986, **149**, 389
- Tvaroska, I. and Kozar, T. *J. Am. Chem. Soc.* 1980, **102**, 6929
- Pavani, R. and Ranghino, G. *Comput. Chem.* 1982, **6**, 133
- Diner, S., Malrieu, J. P., Jordan, F. and Gilbert, M. *Theor. Chim. Acta* 1969, **15**, 100
- Powell, M. J. D. *Computer J.* 1964, **7**, 155
- Zangwill, V. J. *Computer J.* 1965, **8**, 293
- Rees, D. A. *J. Chem. Soc., Part B* 1970, 877
- Rees, D. A. and Scott, W. E. *J. Chem. Soc., Part B*, 1971, 469
- 'The Monosaccharides' (ed. I. Ernest and J. Hebký), Publishing House of the Czechoslovak Academy of Sciences, Prague, 1963
- Rochas, C., Lahaye, M. and Yaphe, W. *Bot. Mar.* 1986, **29**, 335
- Gagnaire, D., Pérez, S. and Tran, V. *Int. J. Biol. Macromol.* 1979, **1**, 42
- Phan Viet, M. T., Lahaye, M., Rochas, C. and Yaphe, W. In preparation
- Rochas, C. and Landry, S. *Carbohydr. Polym.* 1987, **7**, 435
- Pérez, S. and Scaringe, R. P. *J. Appl. Crystallogr.* 1986, **19**, 65